Characterization of grid-oriented control of heat pumps via SG-Ready

Sebastian Beichter, Anne-Christin Süß*, Johannes Galenzowski, Jan Dillmann, Stefan Dietze, Ralf Mikut, Simon Waczowicz, Veit Hagenmeyer*

IAI Institute for Automation and Applied Informatics, Karlsruhe, Germany
** sebastian.beichter@kit.edu, anne-christin.suess@kit.edu, equal contribution*

Keywords: HEAT PUMP, SMART GRID READY, FLEXIBILITY, GRID-ORIENTED CONTROL

Abstract

The integration of heat pumps into energy systems is critical for decarbonisation, with growing installations necessitating their alignment with power grid demands. Heat pump penetration poses challenges for low-voltage grids, such as voltage drops and overloading, while technologies like the SG-Ready interface offer the potential for flexibility and grid-oriented control. However, gaps persist in experimental validation and high-resolution analyses of heat pump behaviour. This study evaluates the dynamic response of two heat pumps using field measurements with 0.2s resolution, focusing on SG-Ready state changes. By openly sharing our dataset, this study advances research on practical applications of grid-oriented control. Results reveal rapid, predictable responses during blocking events but significant variability during start-up, limiting simultaneity in grid operations.

1 Introduction

The rapid growth of heat pump installations has become a key focus for the German government. The Federal Ministry for Economic Affairs and Climate Action aims to install at least 500,000 new units annually starting in 2024, marking a significant step toward decarbonisation [1].

Increasing heat pump penetration significantly impacts low-voltage grids, causing voltage drops and cable overloading. These issues emerge as early as 20–30 % penetration, highlighting the need for grid reinforcements and optimized load management [2]. The German Energy Industry Act §14a enables the grid-oriented control of controllable devices as a stabilization measure. Under this regulation, heat pumps with an electrical connection capacity exceeding 4.2 kW are controllable devices [3]. Since 2012, heat pumps labelled Smart Grid Ready (SG-Ready or SGR), have featured defined interfaces for load management within Germany, Switzerland and Austria [4]. Since January 1, 2025, only heat pumps with interfaces enabling automated, grid-supportive operation, such as SG-Ready or VHPReady, and compatibility with certified Smart-Meter-Gateways qualify for subsidies, ensuring compliance with energy and metering regulations [5].

In this context, Beichter et al. [6] emphasize that high-resolution measurements are vital for operating controllable devices as a stabilization measure, since 15-minute intervals fail to capture critical dynamics during sudden load changes. Sub-minute precision is crucial to evaluate the impacts of grid-oriented control actions, including practical implementations using established interfaces such as SG-Ready [6].

1.1. Related work

Literature, such as the study by Akmal et al. [7], demonstrates that transient voltage issues are a critical concern in low-voltage grids with increasing heat pump penetration, emphasizing the need to understand heat pump-induced system dynamics.

Other research investigates grid-oriented operation by providing Frequency Containment Reserve [8]. This study of Posma et al. demonstrated the potential for grid stability by adjusting power consumption of an aggregation of 20,000 residential heat pumps on a 5-minute timescale. However, the study relies on modelled data and does not validate whether existing SG-Ready heat pumps can implement these strategies, exposing a gap in proving practical capabilities for real-world integration.

Conversely, numerous studies have explored the implementation of control schemes leveraging the SG-Ready interface. Baraskar et al. [9] analysed a PV-battery-heat pump system over 12 months using 1-minute resolution data, focusing on SG-Ready control to maximize PV self-consumption but noted efficiency losses due to temperature increases. An analysis of the system's behaviour at sub-minute resolution is absent.

Göbel et al. [10] demonstrated a significant improvement in PV energy self-consumption, increasing it from 47 % to 63 %, and a reduction in heating costs by up to 30 % through dynamic system control. However, they found that the reliance on binary-state SGR interfaces limits operational flexibility. Overall, this work highlights the need for real-world studies to optimize system controllers in the building sector using interfaces available on the market, like SG-Ready.

Thorsteinsson et al. [11] focused on extending the academic definition of smart grid readiness by demonstrating heat reference tracking using model predictive control. However, their approach does not address the practical operation and limitations of heat pumps found in real-world applications.

Fischer et al. [12] presented a simulation-based control framework for aggregating residential heat pumps using the SG-Ready interface. Their study highlighted the potential of managing large pools to optimize electricity usage and price

fluctuations. However, it lacks experimental validation of heat pump reactions and does not address the practical implications of its control strategies on individual heat pump operations.
The reviewed studies highlight significant gaps in understanding the high-resolution dynamics of heat pumps under SG-Ready control, particularly the lack of sub-minute analyses and limited experimental validation of real-world behaviour. A comprehensive assessment and simulation of the impacts of heat pump integration on grid stability and flexibility requires broader data coverage and higher-resolution measurements than currently available.

1.2. Contribution

To address the challenges identified in the literature, the present study advances the understanding of heat pump behaviour under external control through the SG-Ready interface, emphasizing high-resolution dynamics and real-world applications. Key contributions include:

- **Real-World Validation:** Field measurements evaluated heat pump reactions under realistic conditions, focusing on behaviour during SGR state changes.
- **High-Resolution Measurements:** Data acquisition with 0.2-second resolution to capture fine-grained dynamic events, provided as open data.
- **Repetition for Reliability:** High number of repetitions, with 15-17 repetitions for the same grid control event, to ensure statistical robustness and reliability.
- **Quantification of Simultaneity Effects:** Present state change aligned load profiles during grid control events including a statistical evaluation of reaction times.

This comprehensive approach bridges the gaps in previous studies, providing a deeper understanding of the dynamic and practical integration of heat pumps in grid-oriented systems.

2. Methodology

The methodology section outlines the equipment setup, including the experimental buildings and hardware configuration, the implementation of SG-Ready-based control for the heat pumps, and the study design, detailing the required experiments.

2.1. Equipment setup

The hardware used in the present study consists of two experimental buildings from the Living Lab Energy Campus (LLEC) [6] at the Energy Lab [13] of the Karlsruhe Institute of Technology. One building has an air-to-water heat pump (HP 1), while the other features a ground-source heat pump (HP 2). Both experimental buildings are equipped with a 1000-liter Thermal Energy Storage System (TESS), whose maximum temperatures are set to 46 °C as a supply for space heating. The control commands are executed via a custom-built relay box and the SG-Ready-interface of the heat pump, while status changes are simultaneously transmitted to a database (see Figure 1). In parallel, real-time active power measurements at the heat pump's connection point are recorded every 0.2 s using Janitza UMG 604 Pro devices.

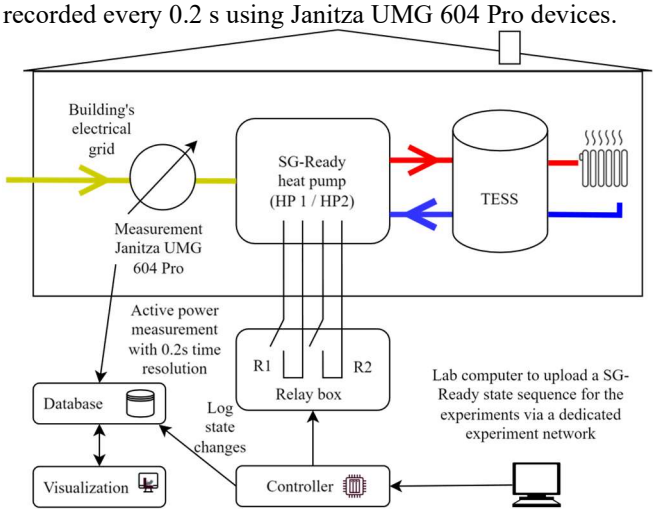

Figure 1: Identical setup for HP1 and HP2 connected to a Thermal Energy Storage System (TESS) controlled by a local controller using a relay box and a measurement database.

2.2. SG-Ready-based control

The varied parameters in this study's design are the four SGR states. The states are set via the two relays in the relay box, R1 and R2 (see Figure 1), which can be automatically triggered for the experiments. According to the technical specifications [4], the expected reaction in the respective states is:

- **Blocking Mode in SGR 1 (R1=1, R2=0):** The heat pump is deactivated for up to two hours. Operational limits, such as the temperature boundaries of the thermal energy storage, are maintained.
- **Normal Operation in SGR 2 (R1=0, R2=0):** The heat pump operates using its default control algorithm.
- **Boosted Operation in SGR 3 (R1=0, R2=1):** The heat pump is recommended to turn on, resulting in increased power demand compared to normal operation.
- **Peak Operation in SGR 4 (R1=1, R2=1)**: The heat pump and any available electric (backup) heaters are activated to maximize power consumption.

2.3. Study design

In grid-oriented operations, emphasis is placed on the SGR state 1, which allows grid operators to temporarily suspend heat pump activity to alleviate grid stress during peak demand periods. To comprehensively assess the system's response, we analyse transitions from all other states 2, 3, and 4 (collectively referred to as SGR state X) to SGR state 1, as well as transitions from SGR state 1 to SGR state X. Using the collection of different states ensures a thorough evaluation of the heat pump's behaviour under various operational conditions.
The same transitions from SGR X to SGR 1 and from SGR 1 to SGR X are executed for each of the heat pumps, HP 1 and HP 2. We restrict the boundary conditions to heating-up events where the storage is not at its limit. The mean ambient

temperature on the respective day is considered the most influential external factor.

A state change is initiated at time t_{signal} which corresponds to the moment the controller sends a signal to the relays. A state change is considered to be complete once a transition into or out of a stationary state is detected. A stationary state is defined as a condition where the difference between two consecutive measurements, smoothed over a moving average of three data points, does not exceed 30 W:

$$t_{stat} = \left\{t \mid \frac{1}{3}\sum_{i=t}^{t+2}|P(i) - P(i-1)| < 30\ W, t > t_{signal}\right\} \quad (1)$$

$$t_{trans} = \left\{t \mid t > t_{signal}, t \notin t_{stat}\right\} \quad (2)$$

When transitioning from SGR X to SGR 1, the reaction time is defined as the duration between the moment the SGR 1 request is sent t_{signal} and the start of the stationary state after the transient. This can be expressed as:

$$t_{react,x\to1} = \min(t_{stat} \mid t_{stat} > \min(t_{trans})) - t_{signal} \quad (3)$$

When transitioning from SGR 1 into SGR X, the reaction time is defined as the duration between the moment the SGR X request is sent t_{signal} and the moment the stationary SGR 1 state is exited, i.e., the last stationary value before the first transient state. This can be expressed as:

$$t_{react,1\to x} = \max(t_{stat} \mid t_{stat} < \min(t_{trans})) - t_{signal} \quad (4)$$

3. Results

The present study shows experiments conducted over five days in November 2024. All recorded state changes are detailed in Table 1. A total of 17 SGR X → 1 state changes were recorded for HP 1 and HP 2, along with 15 SGR 1 → X state changes for HP 1 for HP 2. Only SGR state changes with a power consumption change ($t_{trans} \neq \{\}$) are included in the statistical evaluation, while all measurements that have the potential to react to a state change are displayed in the load profile plots. In Table 1, measurements with a power change are listed before the slash, and the total number after the slash.

Table 1: Daily SG-Ready state changes with significant power shifts for HP 1/HP 2 before the slash, and total changes per day after the slash, and mean ambient temperature (MAT).

	SGR X → 1		SGR 1 → X		MAT
Date	HP 1	HP 2	HP 1	HP 2	in °C
11/21/24	3/3	3/3	2/2	2/2	2.06
11/26/24	4/5	5/5	3/4	4/4	11.10
11/28/24	4/5	5/5	3/5	4/5	9.51
11/29/24	3/4	4/4	4/4	4/4	7.91
Total	14/17	17/17	12/15	14/15	-

The load profiles are shown in Sections 3.1 and 3.2 alongside the statistical evaluation in Section 3.3.

3.1. Transition SGR X → 1

Figure 2 illustrates the recorded load profiles for HP 1, and Figure 3 for HP 2. The power consumption before the transition ranges from 1.8 to 5.2 kW for HP 1 and from 0.4 to 2.6 kW for HP 2. The reaction time $t_{react,x\to1}$ of HP 1 ranges from 0.4 to 2.4 s until the steady state SGR 1 is reached. For HP 2, $t_{react,x\to1}$ ranges from 3.1 to 9.0 s. The response of HP 2 is not only more delayed but also features a ramped reduction over approximately 5 s rather than an almost immediate switch-off like HP 1. In the SGR 1 state, the power consumption is reduced to around 50 W for HP 1 and 100 W for HP 2.

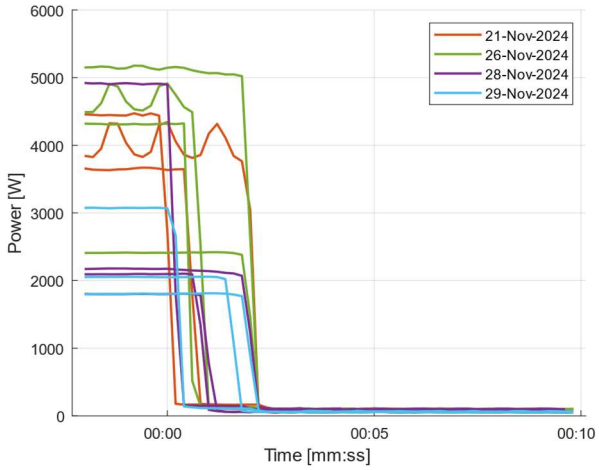

Figure 2: HP 1 transition SGR X → 1, t_{signal} at t = 00:00

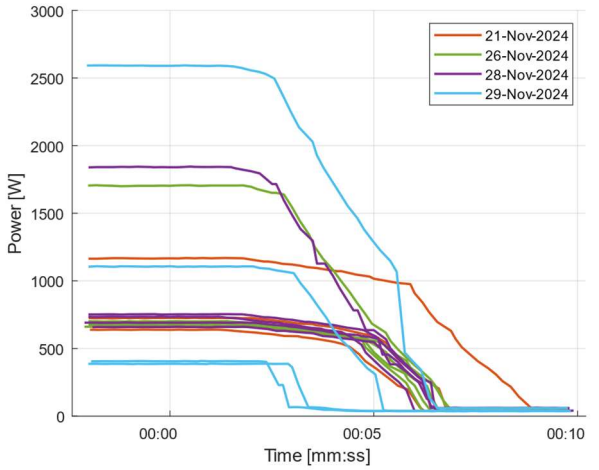

Figure 3: HP 2 transition SGR X → 1, t_{signal} at t = 00:00

3.2. Transition SGR 1 → X

Figure 4 and Figure 5 illustrate the recorded load profiles during a transition from SGR 1 to other SGR states, representing the start-up behaviour after a blocking state. The reaction time $t_{react,1\to x}$ until the SGR 1 state is left, ranges from 1 to 16.5 min for HP 1, and from 3 to 12.7 min for HP 2. When switching on the power consumption of HP 1, it rises to a plateau ranging from 1.5 to 2.4 kW, which is maintained for 2 to 3 min before increasing further for some profiles. Similarly, HP 2 exhibits a plateau between 0.6 to 0.8 kW. In contrast to HP 1, however, the power consumption of HP 2 decreases after the initial plateau, dropping to another plateau in the range of 0.3 to 0.5 kW.

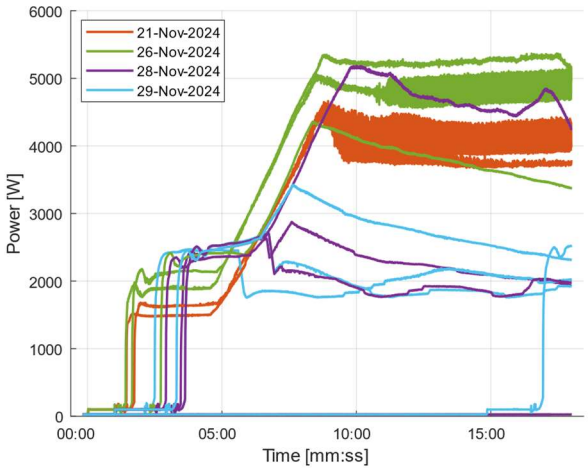

Figure 4: HP 1 transition SGR 1 → X, t_{signal} at t = 00:00

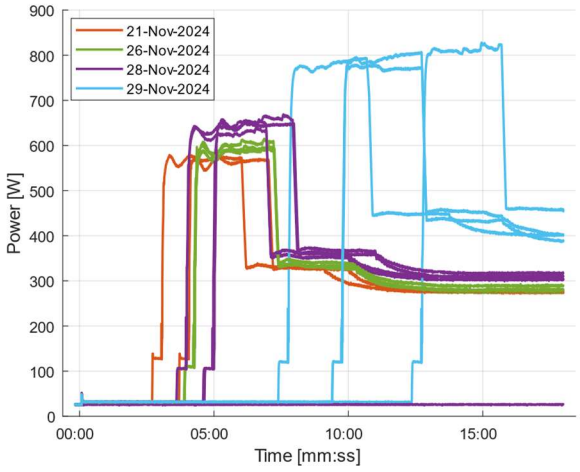

Figure 5: HP 2 transition SGR 1 → X, t_{signal} at t = 00:00

3.3. *Statistical Evaluation*

As displayed in Figure 6 on the left side the stopping times of both heat pumps are presented as violin charts. The median stopping times (marked with a white dot) are 1.3 s for HP 1 and 6.6 s for HP 2. The black boxes with the interquartile range (IQR) contain 50% of the data, ranging from 1.0 to 2.4 s for HP 1 and 6.2 to 6.8 s for HP 2. The black whisker lines represent 1.5 times the IQR, ranging from 0.4 to 2.4 s for HP 1 and 5.4 to 7.1 s for HP 2. The fastest recorded reaction was 0.4 s for HP 1 and 3.1 s for HP 2, while the slowest reaction was 2.4 s for HP 1 and 9.0 s for HP 2.

Figure 6 on the right side shows the start-up times of both heat pumps following the state change from SGR 1 to SGR X. The median reaction times are 146.6 s for HP 1 and 255.3 s for HP 2. The IQR for HP 1 ranges from 78.4 to 189.4 s, and for HP 2, it ranges from 242.4 to 262.4 s. The fastest recorded reaction was 60.1 s for HP 1 and 182.4 s for HP 2, while the slowest reaction was 989.7 s for HP 1 and 762.2 s for HP 2.

A comparison of both HPs reveals that HP 1 (the air-to-water heat pump) exhibits faster reaction times for the blocking state change (SGR X to SGR 1) by a factor of 5, as well as faster start-up reaction times by a factor of 1.74.

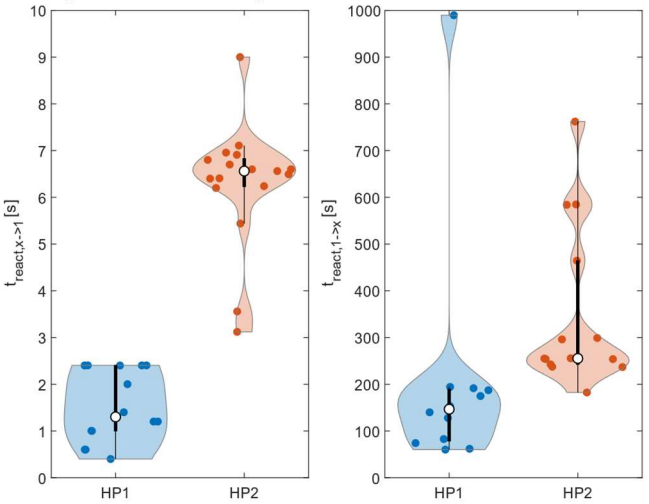

Figure 6: Reaction times of SGR X to SGR 1 state change on the left and SGR 1 to SGR X on the right for HP 1 and HP 2

4. Discussion

This section discusses the observed response times and switching behaviour during grid control events that have caused a change in the power consumption (57/64 SGR state changes), with a focus on their impact on system performance and grid stability. For external control of the heat pumps in a grid-friendly manner it is essential to look at the simultaneity behaviour of the heat pumps. This can be characterized by the reaction times when changing the SGR-state. When looking at the reaction times, we cannot observe any simultaneity behaviour when changing from SGR 1 to SGR X. The median between the two heat pumps differs by a factor of about 1.7. Even within the results of the respective heat pump, the IQRs are very large. When changing from SGR 1 to SGR X, we could not detect any instantaneous switching on. Instead, the time until the switch-on process takes place is in the range of minutes, so that the probability of simultaneous operation with other systems is reduced. These findings, together with the published dataset from this study, provide a robust baseline for advancing forecasting methods, as illustrated by Semmelmann [14], and for refining grid-oriented control strategies.

We observe a rapid ramped behaviour for the change from SGR X to SGR 1. HP 1 transitions to the switched-off state after a median of 1.3 s and HP 2 after 6.6 s. Thus, the switch-off process takes place in the lower seconds range, but there is a spread in both heat pumps. This allows the grid operator to perform a planned ramp-down.

5. Conclusion and Outlook

The present paper systematically examines the electrical behaviour of two heat pumps of different designs when controlled by the SGR signal. For this, tests were carried out on different days with different outside temperatures to

determine how the electrical power consumption behaves when the SGR signal is set, both when the heat pump is blocked and when it starts up, in terms of reaction times and power consumption level. It was found that both heat pumps show a very fast, simultaneous behaviour when blocked. When the heat pumps start up, however, the behaviour of simultaneity does not exist. The reaction times for this are different between and even for the individual heat pumps. The power consumption characteristics also differ between the two heat pumps examined. Thus, it can be concluded for the grid operator that he can expect a rapid constant ramp for the blocking behaviour and that the problem of simultaneity does not arise when switching on, but that it is difficult to predict. Better predictability for the grid operator would be achieved by more precisely defining the behaviour of heat pumps in the label definition when the SGR status changes. The already suspected relationships between the types of different heat pumps should be investigated in further research.

Data available: https://doi.org/10.5281/zenodo.14678762

6. Acknowledgements & Contributions

This project is funded by the Helmholtz Association under the Program "Energy System Design". The authors thank their colleagues from the Institute for Automation and Applied Informatics for all the fruitful discussions and collaborations.

Contributions according to Credit, https://credit.niso.org/:
Conceptualization: S.B., A.S., S.W., J.G.; *Methodology*: S.B., A.S, J.G.; *Software*: S.B., A.S, J.D., S.D.; *Investigation*: S.B., A.S, J.G.; *Data curation*: S.B., A.S; *Writing - original draft*: S.B., A.S, J.G., S.W.; *Writing - review and editing*: S.B., A.S, J.G., S.W., R.M, V.H.; *Visualization*: S.B., A.S, J.G.; *Supervision*: S.W., R.M., V.H.; *Funding acquisition*: V.H.

7. References

[1] Bundesministerium für Wirtschaft und Klimaschutz, "Überblickspapier: Das Klimaschutz-Programm 2023." Oct. 04, 2023. Accessed: Dec. 20, 2024. [Online]. Available: https://www.bmwk.de/Redaktion/DE/Downloads/U/ueberblickspapier-klimaschutzprogramm.pdf

[2] C. Protopapadaki and D. Saelens, "Heat pump and PV impact on residential low-voltage distribution grids as a function of building and district properties," *Applied Energy*, vol. 192, pp. 268–281, Apr. 2017, doi: 10.1016/j.apenergy.2016.11.103.

[3] Bundesnetzagentur, *Beschluss der Beschlusskammer 6 - BK6-22-300, Bonn*, 2023.

[4] Bundesverband Wärmepumpe e.V., "Regularium für das Label 'SG Ready' für elektrische Heizungs- und Warmwasserwärmepumpen." BWP Marketing & Service GmbH, Jun. 01, 2020. Accessed: Jan. 07, 2025. [Online]. Available: https://www.waermepumpe.de/fileadmin/user_upload/bwp_service/Guetesiegel/2020_SG-ready_Regularien_2.0_final.pdf

[5] Bundesministerium für Wirtschaft und Klimaschutz, "Richtlinie für die Bundesförderung für effiziente Gebäude – Einzelmaßnahmen (BEG EM)." Dec. 21, 2023. Accessed: Dec. 20, 2024. [Online]. Available: https://www.bafa.de/SharedDocs/Downloads/DE/Energie/beg_richtline_beg_em_20231221_PDF.pdf

[6] S. Beichter *et al.*, "Towards a Real-World Dispatchable Feeder," in *2023 8th IEEE Workshop on the Electronic Grid (eGRID)*, Karlsruhe, Germany: IEEE, Oct. 2023, pp. 1–6. doi: 10.1109/eGrid58358.2023.10380834.

[7] M. Akmal, B. Fox, J. D. Morrow, and T. Littler, "Impact of heat pump load on distribution networks," *IET Generation, Transmission & Distribution*, vol. 8, no. 12, pp. 2065–2073, Dec. 2014, doi: 10.1049/iet-gtd.2014.0056.

[8] J. Posma, I. Lampropoulos, W. Schram, and W. van Sark, "Provision of Ancillary Services from an Aggregated Portfolio of Residential Heat Pumps on the Dutch Frequency Containment Reserve Market," *Applied Sciences*, vol. 9, no. 3, Art. no. 3, Jan. 2019, doi: 10.3390/app9030590.

[9] S. Baraskar, D. Günther, J. Wapler, and M. Lämmle, "Analysis of the performance and operation of a photovoltaic-battery heat pump system based on field measurement data," *Solar Energy Advances*, vol. 4, p. 100047, 2024, doi: 10.1016/j.seja.2023.100047.

[10] S. Göbel, C. Vering, and D. Müller, "Experimental Investigation of Rule-Based Control Strategies for Hybrid Heat Pump Systems Using the Smart Grid Ready Interface," in *Proceedings of ECOS 2022 - The 35th International Conference on Efficiency, Cost, Optimization, Simulation and Environmental Impact of Energy Systems*, Copenhagen, Denmark, Jul. 2022, pp. 1175–1186. doi: 10.11581/dtu.00000267.

[11] S. Thorsteinsson, H. Cai, J. D. Bendtsen, P. Heer, and J. Vivian, "Making an air-source heat pump smart-grid ready," *J. Phys.: Conf. Ser.*, vol. 2600, no. 5, p. 052006, Nov. 2023, doi: 10.1088/1742-6596/2600/5/052006.

[12] D. Fischer, T. Wolf, and M.-A. Triebel, "Flexibility of heat pump pools: The use of SG-Ready from an aggregator's perspective," presented at the 12th IEA Heat Pump Conference, Rotterdam, 2017.

[13] F. Wiegel, J. Wachter, M. Kyesswa, R. Mikut, S. Waczowicz, and V. Hagenmeyer, "Smart Energy System Control Laboratory – a fully-automated and user-oriented research infrastructure for controlling and operating smart energy systems," *at - Automatisierungstechnik*, vol. 70, no. 12, pp. 1116–1133, Dec. 2022, doi: 10.1515/auto-2022-0018.

[14] L. Semmelmann, M. Hertel, K. J. Kircher, R. Mikut, V. Hagenmeyer, and C. Weinhardt, "The impact of heat pumps on day-ahead energy community load forecasting," *Applied Energy*, vol. 368, p. 123364, Aug. 2024, doi: 10.1016/j.apenergy.2024.123364.